

# A phase transition in acoustic propagation in 2D random liquid media

Emile Hoskinso\* and Zhen Ye

Department of Physics and Center for Complex Systems, National Central University, Chung-li, Taiwan, ROC  
(June 10, 1999)

Acoustic wave propagation in liquid media containing many parallel air-filled cylinders is considered. A self-consistent method is used to compute rigorously the propagation, incorporating all orders of multiple scattering. It is shown that under proper conditions, multiple scattering leads to a peculiar phase transition in acoustic propagation. When the phase transition occurs, a collective behavior of the cylinders appears and the acoustic waves are confined in a region of space in the neighborhood of the transmission source. A novel phase diagram is used to describe such phase transition.

When propagating through media containing many scatterers, waves will be scattered by each scatterer. The scattered wave will be again scattered by other scatterers. Such a process will be repeated to establish an infinite recursive pattern of multiple scattering, effectively causing the scattering characteristics of the scatterers to change. Multiple scattering of waves is responsible for many fascinating phenomena [1], including modulation of ambient sound at ocean surfaces [2], acoustic scintillation from turbulent flows [3], white paint, random lasers [4], electrical resistivity, and photonic band gaps in periodic structures [5]. More interesting, perhaps, under proper conditions multiple scattering leads to the unusual phenomenon of wave localization, a concept introduced by Anderson [6] to explain the conductor-insulator transition induced by disorders in electronic systems. That is, the electrical conductivity can be completely blocked and electrons remain localized in the neighborhood of the initial emission site due to multiple scattering of electronic waves by a sufficient amount of impurities in solids. By analogy, it has been conjectured that similar localization effect may also exist in the transmission of classical waves in randomly scattering media.

Considerable efforts have been devoted to propagation of classical waves in random media. Localization effects have been reported for microwaves in 2D random systems [7], for acoustic waves in underwater structures [8], and for light [9]. Research also suggests that acoustic localization may be observed in bubbly liquids [10,11]. Despite the efforts, however, no deeper insight into localization can be found in the literature, as suggested by Rusek *et al.* [12]. The general cognition is that enhanced backscattering is a precursor to localization and waves are always localized in 2D random systems. Important questions such as how localization occurs and manifests remain unresolved. It is also unknown how many types of localization exist. It is believed that localization is a phase transition. However, how to characterize such a phase transition has not been considered in the literature. A deeper question may concern whether wave localization corresponds to a symmetry breaking and whether the collective behavior often seen in phase transitions such as superconductivity exists. This paper attempts to shed light on these questions.

In this paper, we present a rigorous study of acoustic propagation in liquid media containing many air-filled cylinders. The approach is based upon the self-consistent theory of multiple scattering [13] and has been used previously to study acoustic localization in bubbly liquid media [11]. Wave propagation is expressed by a set of coupled equations and is solved rigorously. We report a new phase transition in acoustic localization in 2D random liquids that not only waves are confined near the transmitting source but an amazing collective phenomenon emerges. Unlike previous 2D cases, waves are not always localized. An essential component of localization in this case arises from the natural resonance and the collective behavior of the cylinders.

We consider a 2D acoustic system in the cylindrical coordinates shown in Fig. 1. Assume that  $N$  uniform air-cylinders of radius  $a$  are placed randomly in parallel in water perpendicular to the  $x - y$  plane, forming a random cylindrical array. All cylinders are placed within a circle of radius  $R$ ; the cylinder numerical density is  $N/(\pi R^2)$ . The fraction of area occupied by the cylinders per unit area  $\beta$  is  $Na^2/R^2$ ; the average distance between nearest neighbours is therefore  $(\pi/\beta)^{1/2}a$ . No cylinder is located at the origin, where a line source is placed, and no two cylinders can occupy the same spot, i. e. hard sphere approximation. Experimentally, the air-cylinders can be any gas enclosure with a thin insignificant elastic layer, like the Alunex bubbles used in echocardiography [14]. We investigate the acoustic propagation in such random liquid media.

---

\*Address after July 1, 1999: Department of Physics, University of California, Berkeley, CA, USA

A unit acoustic line source, transmitting monochromatic pressure waves, is set at the origin, also perpendicular to the  $x - y$  plane. Due to the large contrast in acoustic impedance between air and water, the air-cylinders are strong acoustic scatterers. Unlike the spherical bubble case, the absorption caused by thermal exchange and viscosity is unimportant here and can be ignored [15].

Multiple scattering in such systems can be computed exactly using the well-known self-consistent method [13] and the matrix inversion scheme [11]. In the scheme, the multiple scattering can be solved in terms of the response function of individual scatterers.

The response function of the single cylinder denoted by  $\Pi_i$  is readily computed by the modal-series expansion in the cylindrical coordinates [16,17]; for the present case,  $\Pi_1 = \Pi_2 = \dots = \Pi_N$ . It is found that strong response from a single cylinder occurs for  $ka$  ranging roughly from 0.0005 to 0.5, and a resonant peak is located at  $ka$  around 0.005; here  $k$  is the conventional wavenumber and  $a$  is the radius of the cylinders. In this range of  $ka$ , to which our attention is restricted, the radial pulsation of the cylinders, i. e. the monopole mode, dominates the scattering. In this case, the scattering from any single cylinder is isotropic in the  $x - y$  plane. The scattering function is plotted against frequency in Fig. 2, where both real and imaginary parts of the scattering function are plotted. The scattering cross section of a single cylinder reaches a peak. For frequencies above the peak, although it reaches a minimum, the scattering function does not vary much.

Consider that the cylinders are located at  $\vec{r}_i$  ( $i = 1, 2, \dots, N$ ) in the cylindrical coordinates. The scattered wave  $p_s$  from each cylinder, the  $i$ -th say, is a linear response to the incident wave composed of the direct incident wave from the source and *all* scattered waves from other cylinders.

Similar to the 3D case [11], the scattered wave from the  $i$ -th cylinder is therefore

$$p_s(\vec{r}, \vec{r}_i) = \Pi_i \left( p_0(\vec{r}_i) + \sum_{j=1, j \neq i}^N p_s(\vec{r}_i, \vec{r}_j) \right) \times i\pi H_0^{(1)}(k|\vec{r} - \vec{r}_i|), \quad (1)$$

where the second term on the RHS refers to the multiple scattering, and  $p_0$  is the direct incident wave from the source and equals the usual 2D Green's function for a unit line source, i. e.  $i\pi H_0^{(1)}(k|\vec{r}|)$ ; here  $H_0^{(1)}$  is the zero-th order Hankel function of the first kind. To solve for  $p_s(\vec{r}_i, \vec{r}_j)$ , we set  $\vec{r}$  at one of the scatterers. Then Eq. (1) becomes a set of closed self-consistent equations and can be solved by matrix inversion. Once  $p_s(\vec{r}_i, \vec{r}_j)$  is determined, the total wave at any space point is given by

$$p(\vec{r}) = p_0(\vec{r}) + \sum_{i=1}^N p_s(\vec{r}, \vec{r}_i). \quad (2)$$

First consider wave transmission through the media as a function of frequency. We plot the ratio  $|p(\vec{r})|^2/|p_0(\vec{r})|^2$  in the limit  $|\vec{r}| \rightarrow \infty$ , giving the far field transmitted intensity. A set of numerical computations has been performed for various area fractions  $\beta$ , numbers  $N$ , and dimensionless  $ka$ . All parameters are non-dimensionalized. Distances have units of the unspecified constant  $a$  and functions are dependent only on the dimensionless parameter  $ka$  rather than  $k$  and  $a$  independently. Figure 3 presents one of the typical results for the transmitted intensity in a given direction as a function of frequency in terms of  $ka$  the air-cylinder distribution shown in Fig. 1. It is shown that the transmission is significantly reduced from  $ka = 0.006$  to  $ka = 0.02$ ; little energy is transmitted through. Outside this frequency region, however, there is no significant propagation inhibition; transmitted intensity varies around the value one. This result holds for any directions of transmission, i.e. it is representative of the frequency dependence of the total power escaping to infinity. In line with the 3D situation [11], the regime in which the transmission is blocked indicates acoustic localization and is referred to as the localization regime. When  $N$  is increased while keeping  $\beta$  constant, the transmitted intensity for  $ka$  between 0.006 and 0.02 will decrease as  $\exp(-(N/\beta)^{1/2}/(L_a/a))$ , from which the energy localization length  $L_a$  can be estimated in terms of the cylinder radius  $a$ . Note from Fig. 3 that at certain frequencies, the transmission is enhanced. Such enhancement can be due to strong scattering of individual bubbles, multi-reflection at the sample boundary, or the strong multiple scattering among scatterers in certain directions, but it is not due to a global collective behavior of the scatterers. We also note that the localization does not occur at the resonance peak located at around  $ka = 0.005$ .

To further explore the behavior of acoustic localization in such systems, we investigate the response of each individual cylinder to the incident waves. Upon incidence, each cylinder acts effectively as a secondary source. The scattered wave can be regarded as the sum of the radiated waves from these secondary sources. From Eq. (1), the contribution from a given cylinder may be rewritten as

$$p_s(\vec{r}, \vec{r}_i) = i\pi A_i H_0^{(1)}(k|\vec{r} - \vec{r}_i|), \quad (i = 1, 2, \dots, N), \quad (3)$$

where the complex coefficient  $A_i$  denotes the effective strength of the secondary source and is computed incorporating *all* multiple scattering effects. Note that without the scatterers, obviously we will have  $A_i = \Pi_i p_0(\vec{r}_i) = i\pi\Pi_i H_0^{(1)}(k|\vec{r}_i|)$ .

We express  $A_i$  as  $|A_i|\exp(i\theta_i)$ : the modulus  $A_i$  represent the strengths, whereas  $\theta_i$  refer to the phase of the effective secondary sources. We assign a unit vector,  $\vec{u}_i$ , termed the phase vector hereafter, to each phase  $\theta_i$ , and represent these phase vectors by a phase diagram in the  $x - y$  plane: The phase vectors are written as  $\vec{u}_i = \cos\theta_i\vec{e}_x + \sin\theta_i\vec{e}_y$ , where  $\vec{e}_x$  and  $\vec{e}_y$  are unit vectors in the  $x$  and  $y$  directions respectively; in the phase diagram, the phase vector  $\vec{u}_i$  is located at the cylinder to which the phase  $\theta_i$  is associated.

Setting the phase of the initial driving source to zero, numerical experiments are carried out to study the behavior of the phase vectors and energy spatial distribution as the incidence frequency varies. We observe an amazing pattern transition for the phase vectors, with which the wave localization is correlated. The left column of Fig. 3 shows the phase diagram for the phase vectors. The right column shows surface plots of the corresponding secondary source strength magnitudes  $|\vec{r}_i||A_i|^2$ , giving the energy distribution scaled to eliminate geometrical spreading effects. The same cylinder array as in Fig. 1 has been used; three frequencies below, within, and above the localization regime are chosen according to the results in Fig. 3. In this particular case, we have set  $\beta = 10^{-3}$  and  $N = 200$ .

We observe that for frequencies below about  $ka = 0.006$  [18] i. e. for frequencies on the left side of the localization regime indicated by Fig. 4, there is no ordering in the phase vectors  $\vec{u}_i$ . The phase vectors point to various directions. The energy distribution is extended in the  $x - y$  plane, and no acoustic localization appears. These are illustrated by the case of  $ka = 0.0044$  in Fig. 4.

As the frequency increases, an ordering in the phase vectors and the energy localization starts to appear. There is a transition period in which the phase vectors point to either the positive  $x$ -axis or the negative  $x$ -axis, as shown by the case of  $ka = 0.008$ . For frequencies fully within the localization regime indicated by Fig. 3, all phase vectors point to the same direction, implying that all cylinders oscillates completely in phase. As indicated by the cases with  $ka = 0.012$  and  $0.018$  in Fig. 4, all phase vectors point to the negative  $x$ -direction, exactly out of phase with the transmitting source. Such collective behavior allows for efficient cancellation of incoming waves [17]. In this case, the wave energy is localized near the transmitting source. It decays about exponentially in all directions, setting the localization length to be around  $26a$ , much smaller than the range enclosing the random cylinder array; for  $\beta = 10^{-3}$  and  $N = 200$ , the range  $R$  is around  $450a$ . The localization behavior is independent of the outer boundary and always surfaces for sufficiently large  $\beta$  and  $N$ . In the field theory, such a collective phenomenon is an indication of a global behavior of the system and may imply a symmetry breaking and appearance of a kind of Goldstone bosons.

The non-localization at  $ka = 0.0044$  is not caused by the finite sample size, because no indication of energy localization appears as we increase the sample size. If the wave were localized at this frequency, the localization length would be shorter than that for  $ka = 0.012$ , as the scattering is stronger (Fig. 2). The localization would be stronger; this is not observed.

When the frequency increases further, moving near the upper transition edge, the global in-phase ordering starts to disappear. This is illustrated by the case of  $ka = 0.0216$ . When moving out of the localization regime, the in-phase ordering disappears completely. In the meantime, the wave becomes extended again. This is shown by the example  $ka = 0.04$  in Fig. 4.

In Fig. 4, we also plot the phase portraits for three frequencies ( $ka = 0.002, 0.0034$  and  $0.036$ ) at the enhanced transmission shown by Fig. 3. It is shown that there is no apparent phase ordering in these cases. The figure also show that the enhancement in one direction does not necessarily imply enhancement in all directions.

To quantify the phase transitions shown in Fig. 4, we may define two tentative order parameters. For the in-phase behavior, the magnitude of the summation of all phase vectors normalized by  $N$  may be regarded as a phase order parameter, called order parameter 1. For the mixed ordering shown in the transition regime, we may define the order parameter as  $\frac{1}{N} \sum_i^N (|u_x(i)| - |u_y(i)|)$ , termed order parameter 2. These order parameters are plotted as a function of frequency in Fig. 5. When all cylinders oscillate in phase, the order parameter 1 is close to one, while in the transition regime, the order parameter 2 may be more proper in describing the phase transition.

The behavior of the system is a result of the interplay between the single cylinder scatter function and the many body interactions. Without multiple scattering, the localization and coherence phenomenon does not occur. Both the phase and strength of the scattering function determine how a multiply scattered wave propagates through the medium. Exactly how the interplay between the scattering function and the multiple scattering gives rise to the localization and the global coherence behavior remains an open question and may only be understood by an analytic analysis which is under our consideration.

The localization or the transmission drop starts at a frequency slightly above the resonant peak, about the minimum of the imaginary scattering function. Throughout the localization regime, the scattering function varies mildly. The localization or the transmission drop disappears at some frequency which does not appear to be dependent on the peak or the dip of the scattering cross section. The phase transition at the lower frequency edge seems to be related

with the small dip in the scattering cross section or in the imaginary part of scattering function, while the transition at the higher end to the decreasing wavelength. Once the cylinders become too many wavelengths apart, despite a slight increase in the strength of the scattering cross section, phase coherence can no longer be maintained and localization is destroyed.

We have modified the scattering function manually, and observed that transmission is sensitive to it. If, however, the scattering function is held constant at its value for a frequency within the localized range, and the transmission calculated versus frequency using this constant value, the phase transitions and a similar transmission behavior are still observed.

The following considerations support and elucidate the localization behaviour and phase transition observed. (1) The localization is not due to dissipation. Acoustic absorption is negligible in the cases considered, and no mechanism for absorption has been included in our model. (2) By varying the cylinder number  $N$  while keeping the area fraction  $\beta$  constant, it can be shown that the localization or non-localization behavior is qualitatively unchanged, thus not caused by the boundary of the cylinder arrays. (3) The above localization phenomena are caused by multiple scattering. When we manually turn off the multiple scattering from Eq. (1), the localization disappears. (4) The localization behavior also disappears when the cylinder concentration reaches a sufficiently low level. The localization range in Fig. 3 is narrowed, tending to vanish. (5) When the wave is not localized, the energy distribution varies as the random placement of the cylinders changes at a given concentration  $\beta$ . Once localized, the localization behavior will *not change* as the cylinder placement varies.

In summary, we have demonstrated a new phase transition in acoustic propagation in 2D random arrays of air-cylinders in water. When the concentration of the air-cylinders exceeds a certain value, acoustic waves become localized near the transmitting source within a range of frequencies. The results indicate that the wave localization is related to the collective behaviour of the air-cylinders in the presence of multiple scattering. We take the view that the coherent behavior allows for efficient cancellation of the source wave, giving rise to localization, but localization and coherence occur hand-in-hand and the statement that the localization is due to the coherence or visa-versa may be just a matter of perspective. Although these properties may not hold in general, the fact that they do for resonant air-cylinders makes these scatterers ideal for theoretical and experimental localization studies.

The work received support from National Science Council of ROC and from National Central University in the form of a special scholarship to EH.

- 
- [1] A. Ishimaru, *Wave propagation and scattering in random media*, (Academic Press, New York, 1978).
  - [2] D. M. Farmer and S. Vagle, *J. Acoust. Soc. Am.* 86, 1897 (1989).
  - [3] D. M. Farmer, S. F. Clifford, and J. A. Verall, *J. Geophys. Res.* 92, 5368 (1985).
  - [4] N. M. Lawandy, R. M. Balachandran, A. S. L. Gomes, and E. Sauvain, *Nature* 368, 436 (1994).
  - [5] W. M. Robertson, *et al.*, *J. Opt. Soc. Am. B* 10, 322 (1993).
  - [6] P. W. Anderson, *Phys. Rev.* 109, 1492 (1958).
  - [7] R. Dalichaouch, J. P. Armstrong, S. Schultz, P. M. Platzman, and S. L. McCall, *Nature* 354, 53 (1991).
  - [8] C. H. Hodges and J. Woodhouse, *J. Acoust. Soc. Am.* 74, 894 (1983).
  - [9] D. S. Wiersma, P. Bartolini, A. Lagendijk, and R. Roghini, *Nature* 390, 671 (1997).
  - [10] D. Sornette and B. Souillard, *Europhys. Lett.* 7, 269 (1988).
  - [11] Z. Ye and A. Alvarez, *Phys. Rev. Lett.* 80, 3503 (1998).
  - [12] M. Rusek, A. Orłowski, and J. Mostowski, *Phys. Rev. E.* 53, 4122 (1996).
  - [13] L. L. Foldy, *Phys. Rev.* B67, 107 (1945).
  - [14] N. de Jone and L. Hoff, *Ultrasonics* 31, 175 (1993).
  - [15] D. E. Weston, in *Underwater Acoustics*(ed. V. M. Albers) (Plenum, New York, 1967).
  - [16] T. Hasegawa, *et al.*, *J. Acoust. Soc. Am.* 93, 154 (1993);
  - [17] Z. Ye and E. Hoskinson, *Notes on acoustic localization*, unpublished (1998); Z. Ye and E. Hoskinson, *Localization of acoustic propagation in water with air cylinders*, submitted.
  - [18] For extremely low frequencies our model may not be applicable, but this is not our interest.

## FIGURE CAPTIONS

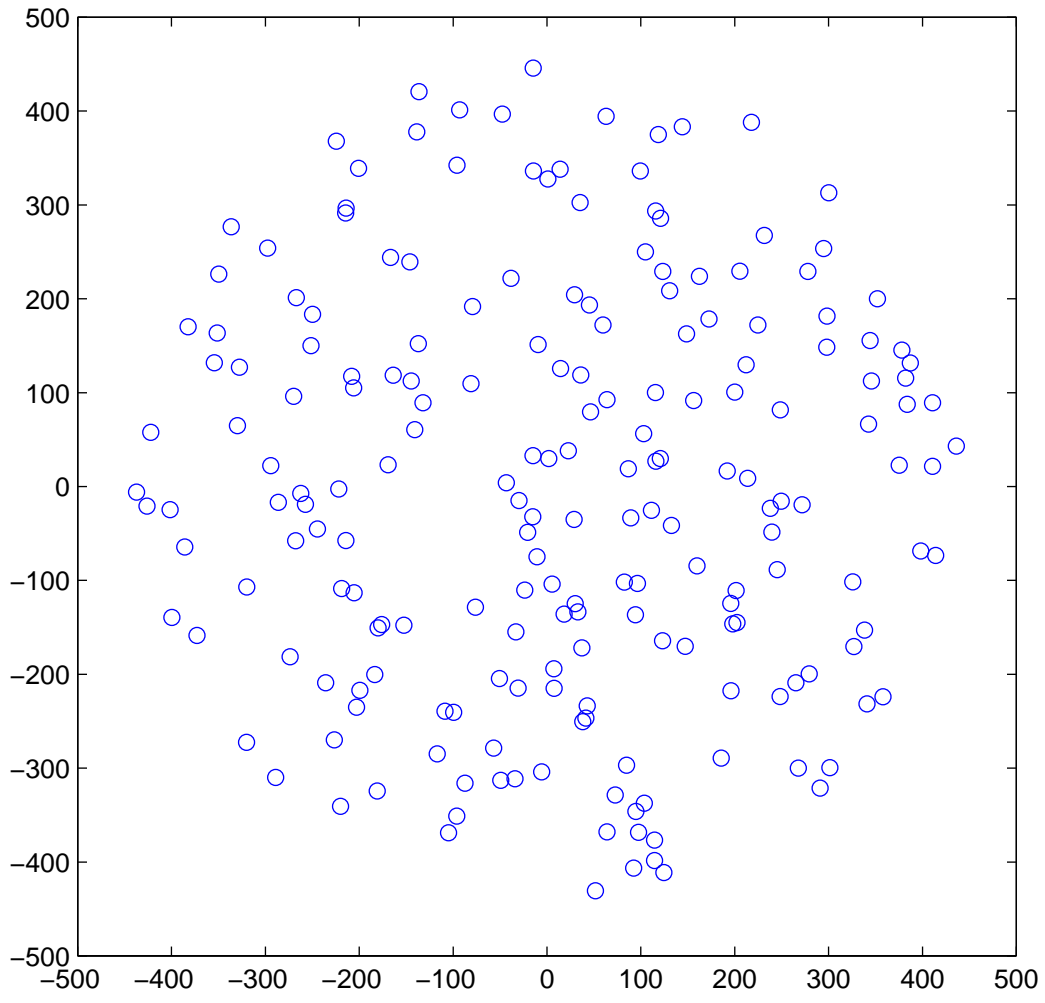
**Fig. 1** Top view of a random distribution of air-cylinders. The circles refer to the air-cylinders (not to scale). A straight line source is placed at the origin.

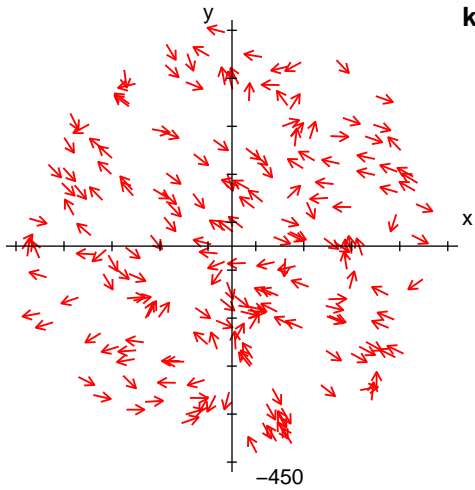
**Fig. 2** The scattering function versus frequency.

**Fig. 3** Transmission versus frequency in terms of  $ka$ .

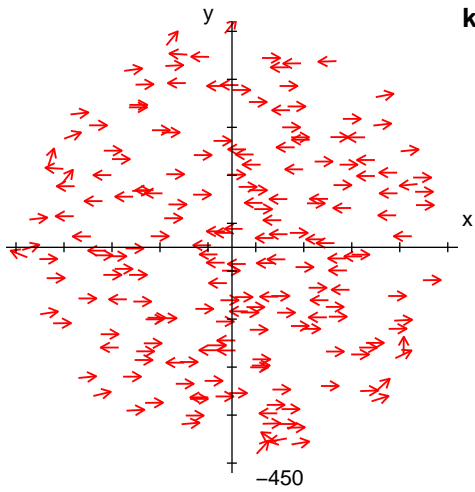
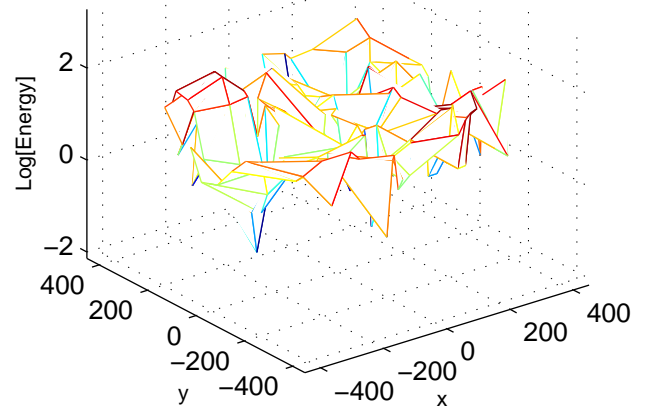
**Fig. 4** Left column: Phase diagram for the two-dimensional phase vector defined in the text. Right column: Spatial distribution of acoustic energy (arbitrary scale).

**Fig. 5** ‘Order parameters’ versus frequency.

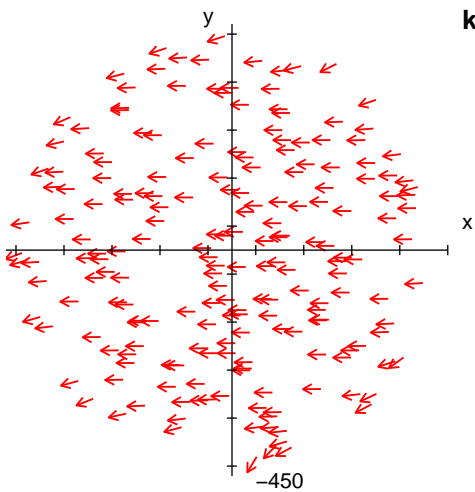
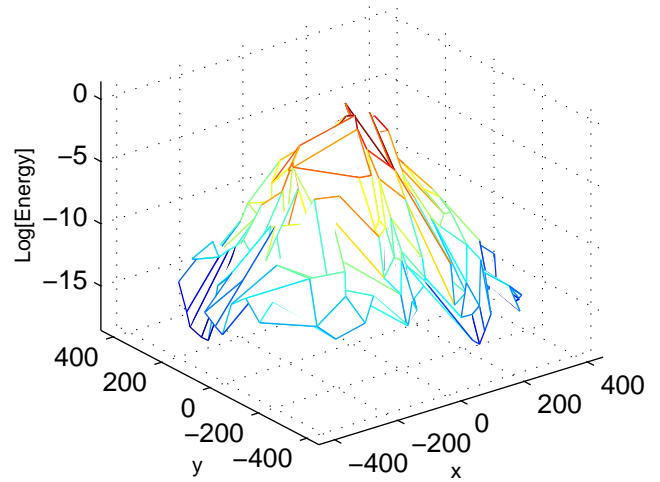




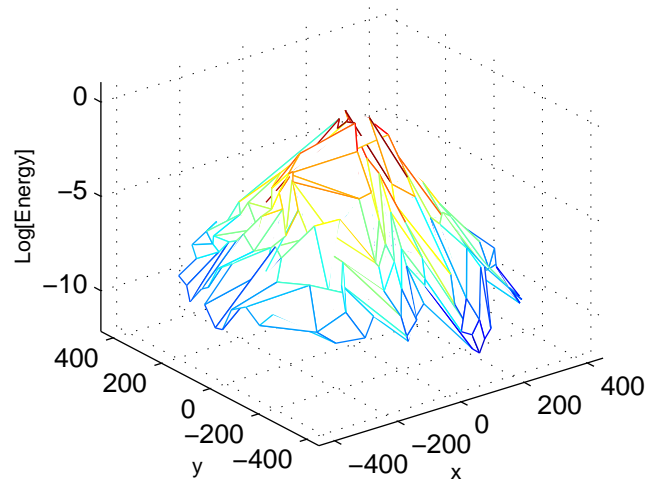
**ka = 0.0044**

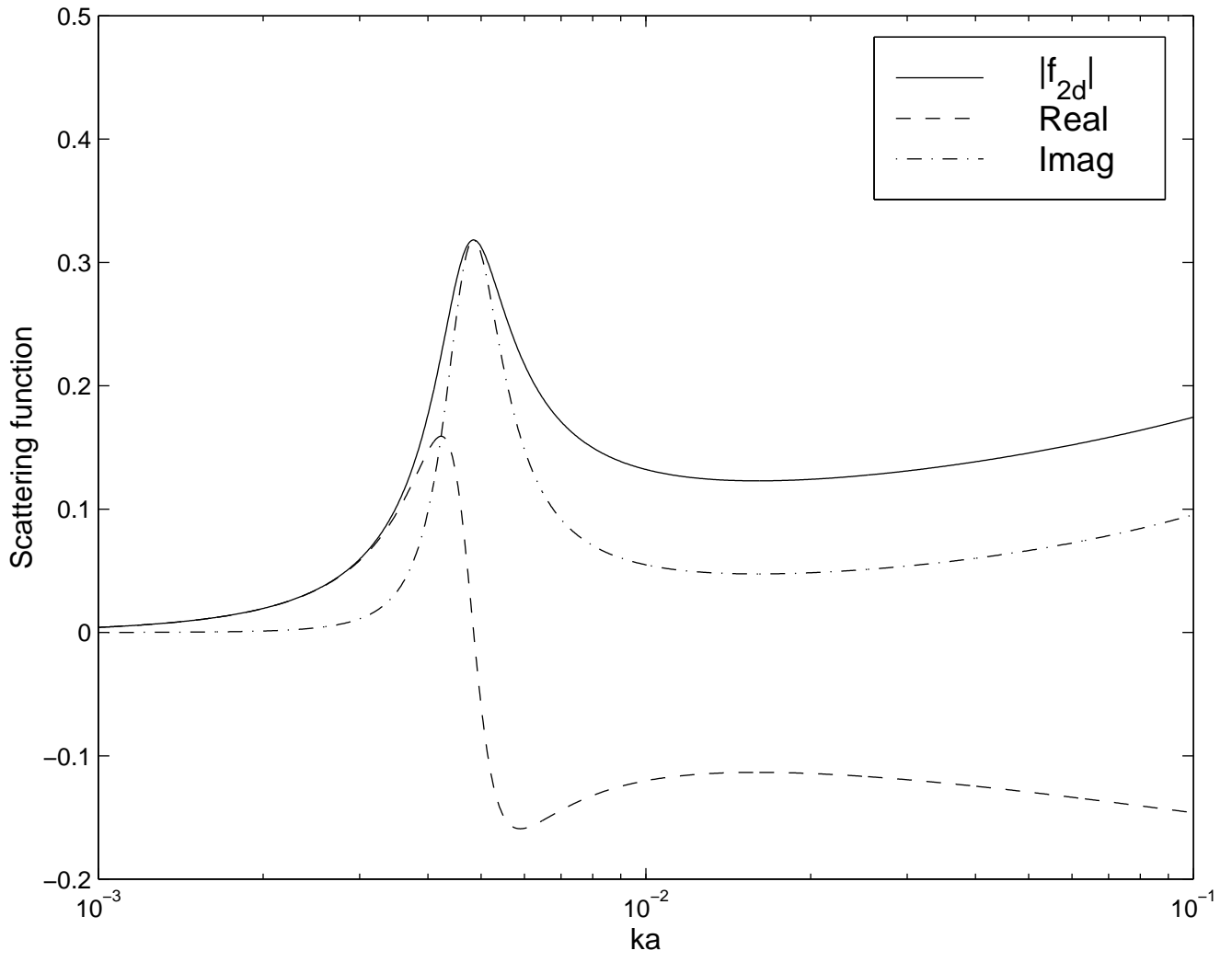


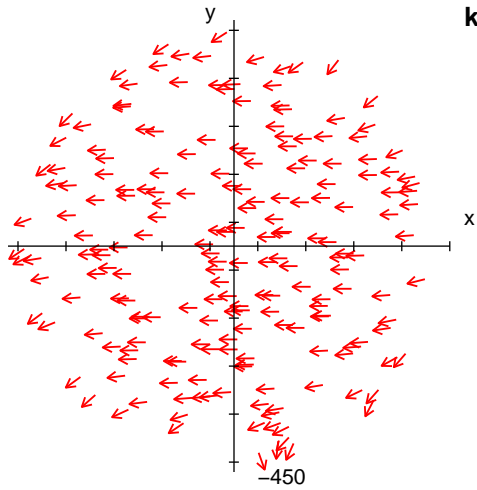
**ka = 0.008**



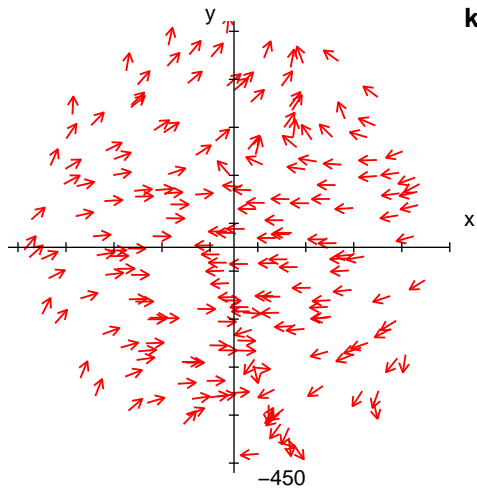
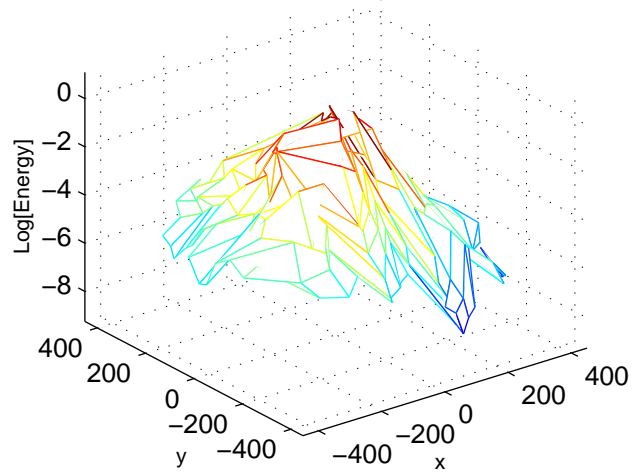
**ka = 0.012**



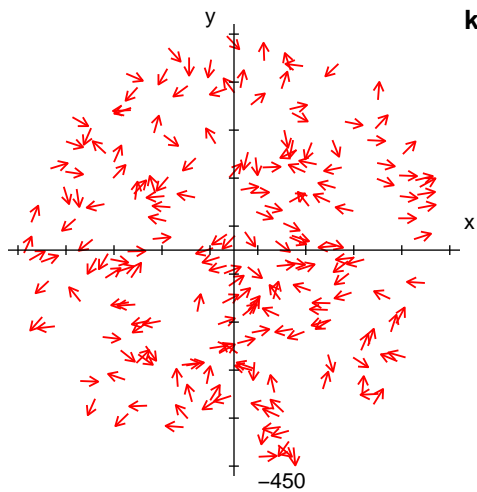
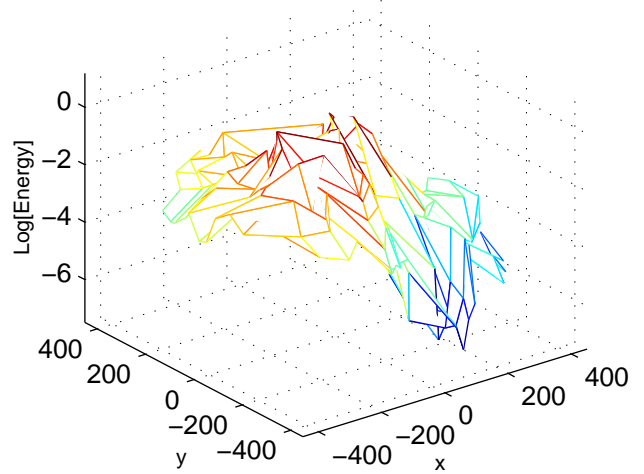




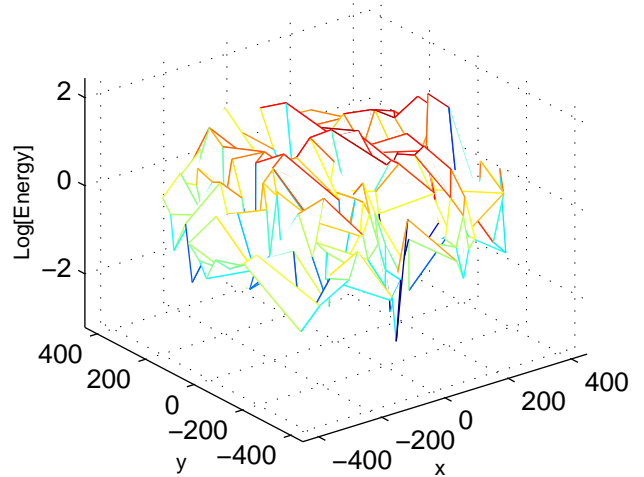
**ka = 0.018**

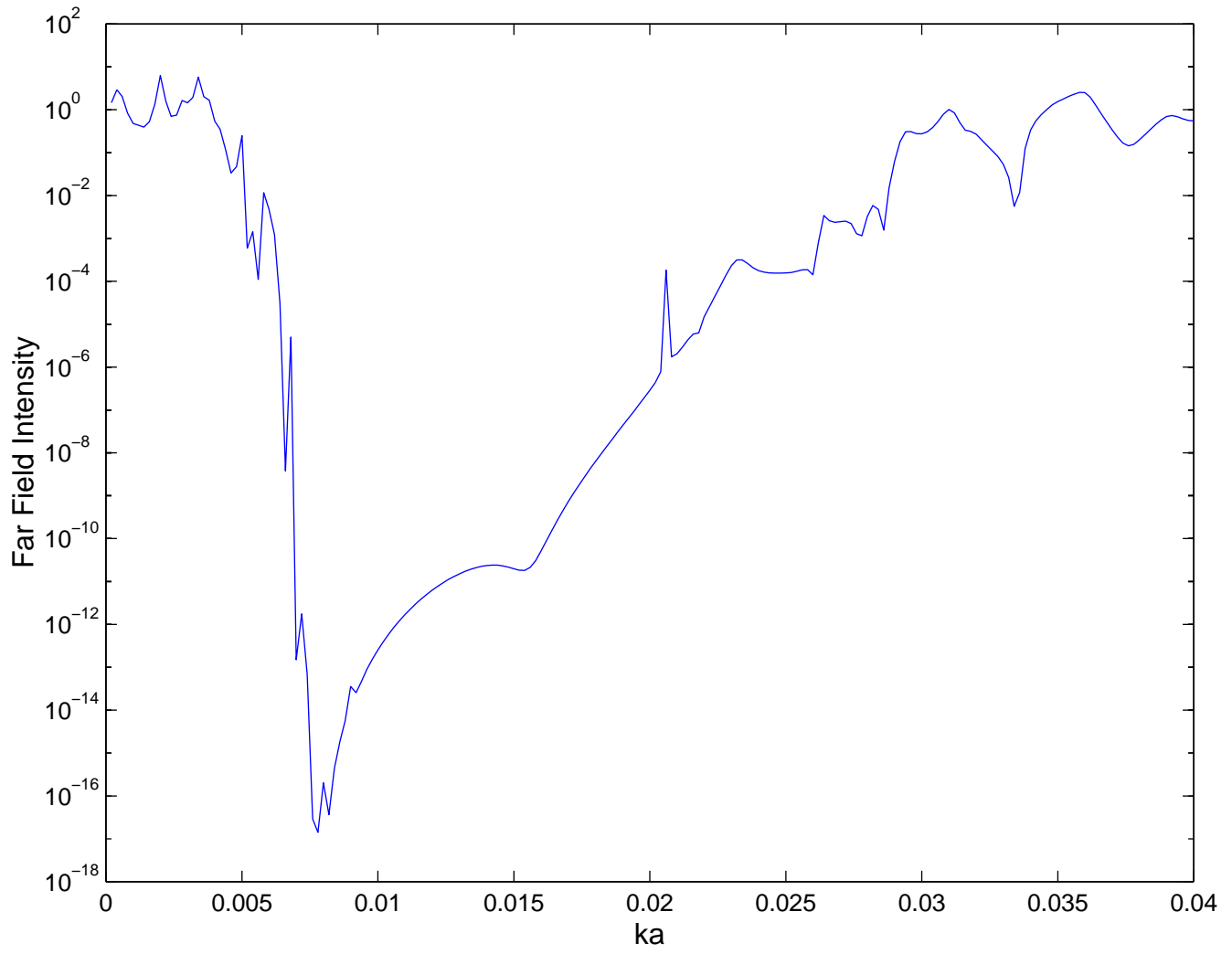


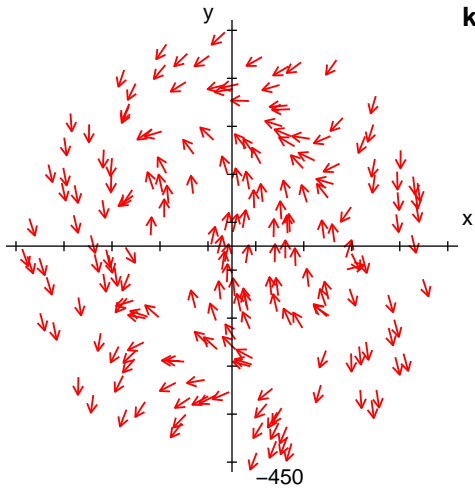
**ka = 0.0216**



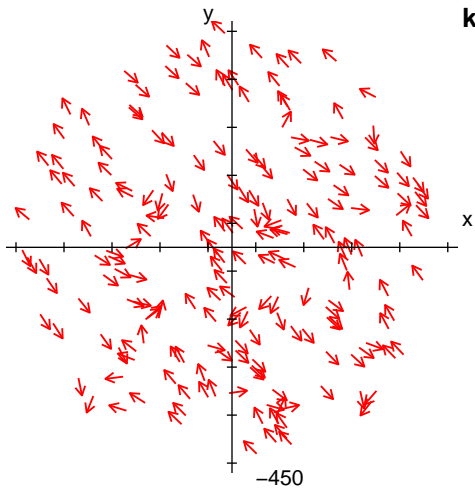
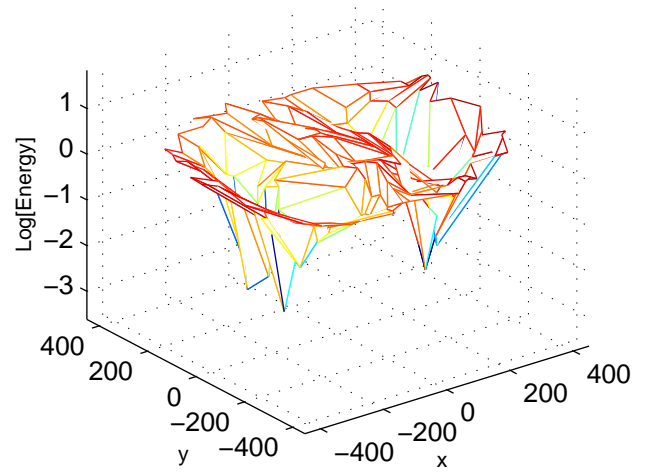
**ka = 0.04**



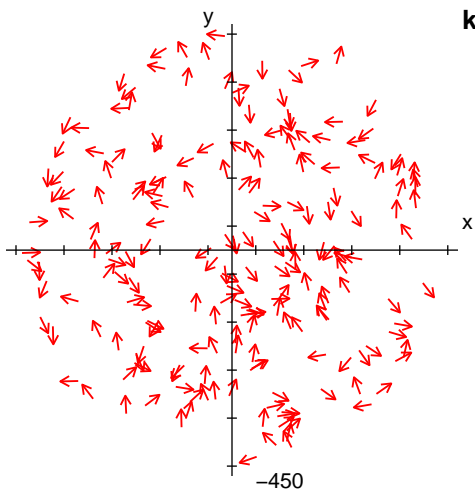
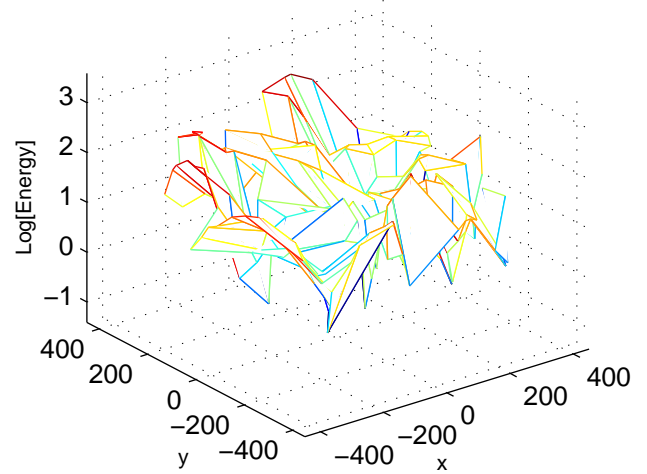




**ka = 0.002**



**ka = 0.0034**



**ka = 0.036**

